All-reflective UV-VIS-NIR transmission and fluorescence spectrometer for µm-sized samples

Friedrich O. Kirchner, Stefan Lahme, Eberhard Riedle, and Peter Baum

Citation: AIP Advances **4**, 077134 (2014); doi: 10.1063/1.4891863
View online: http://dx.doi.org/10.1063/1.4891863
View Table of Contents: http://aip.scitation.org/toc/adv/4/7
Published by the American Institute of Physics

All-reflective UV-VIS-NIR transmission and fluorescence spectrometer for μm-sized samples

Friedrich O. Kirchner,[1,2] Stefan Lahme,[1,2] Eberhard Riedle,[3] and Peter Baum[1,2]
[1]*Max-Planck-Institut für Quantenoptik, Hans-Kopfermann-Str. 1, 85748 Garching, Germany*
[2]*Ludwig-Maximilians-Universität München, Am Coulombwall 1, 85748 Garching, Germany*
[3]*Lehrstuhl für BioMolekulare Optik, Ludwig-Maximilians-Universität München, Oettingenstr. 67, 80538 München, Germany*

(Received 10 March 2014; accepted 21 July 2014; published online 29 July 2014)

We report on an optical transmission spectrometer optimized for tiny samples. The setup is based on all-reflective parabolic optics and delivers broadband operation from 215 to 1030 nm. A fiber-coupled light source is used for illumination and a fiber-coupled miniature spectrometer for detection. The diameter of the probed area is less than 200 μm for all wavelengths. We demonstrate the capability to record transmission, absorption, reflection, fluorescence and refractive indices of tiny and ultrathin sample flakes with this versatile device. The performance is validated with a solid state wavelength standard and with dye solutions. [http://dx.doi.org/10.1063/1.4891863]

I. INTRODUCTION

The study of interaction between light and matter, spectroscopy, is a valuable tool for understanding the structure and function of materials ranging from biological specimens over crystals and liquids to molecules or atoms. Often it is required to measure a spectrum from very tiny objects or microscopic areas of larger samples. Such capability is relevant, for example, in forensics of fabrics or hairs, investigations of laser-damaged spots on mirrors, analysis of bank notes, pixilated displays, protein microcrystals, paintings or mineral inclusions.

The application in our laboratory is the optical characterization of nanometer-thick material films to be used as samples in femtosecond single-electron diffraction,[1–3] for revealing atomic motion in space and time. In such experiments, the energy of the probing electron pulses is about 100 keV and this limits the allowable sample thickness to tens of nanometers. Ideally the films are single-crystalline. Ultramicrotomy, i.e. cutting materials with a diamond knife having a nanometer-sized edge, is a promising approach to produce the required thin-films, but the achievable diameter with this technique is typically limited to hundreds of μm.[4,5] Before ultrafast electron diffraction is attempted, it is mandatory to know the sample's absorption and transmission properties, in order to determine how much pump pulse energy is needed to trigger the desired transition and the resonance wavelength. A spectroscopic apparatus is hence required that works with μm-sized samples, covering the entire relevant spectral range from the ultraviolet over the visible to the near infrared.

Before the general availability of fiber-coupled spectrometers and light sources in the last two decades, setups with a similar application focus had to be constructed from high-power discharge lamps, spatially filtered by a pin hole. The matching detection units were composed of scanning spectrometers. Fiber-based setups with focus on small probing area and quantitative capabilities have not been reported so far. The closest related report we could find is a lens-based technique[6] that obtains spatial resolution only by recording sub-focus sized targets. Here we report on a transmission and fluorescence spectrometer that covers a wavelength range from 215 to 1030 nm and simultaneously provides a focal spot of less than 200 μm in diameter. We apply a fiber-coupled

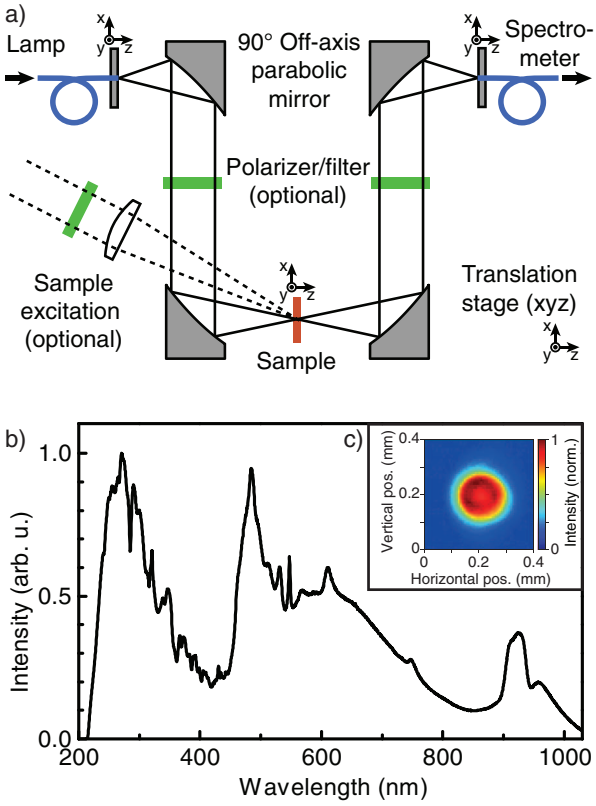

FIG. 1. (a) Schematic of the microspectrometer. Light from a deuterium-tungsten halogen lamp is sent through an optical fiber (blue), the aperture of which is imaged onto the sample (red) by a pair of 90° off-axis parabolic mirrors (grey). The light transmitted through the sample is collected and focused onto the entrance aperture of another fiber (blue). A spectrometer enables spectrally resolved measurements of the transmission. Optional laser excitation (dotted) and polarizers/analyzers (green) allow obtaining polarization-sensitive absorption and fluorescence spectra from micrometer-sized samples. (b) Effective spectrum of the deuterium-tungsten halogen lamp as recorded through the microspectrometer. (c) Focal spot of the microspectrometer at the location of the sample, recorded over all wavelengths.

broadband lamp and a fiber-coupled miniature grating spectrograph in combination with an all-reflective imaging design based on off-axis parabolic mirrors. The setup is almost alignment-free as a result of careful mechanical construction with an optical cage system and the open construction offers ample possibilities for complex experiments. This approach is seemingly simple, but has not been reported so far. We hence deem a detailed description of design and performance useful for application and future advances, especially for such researchers not working in the fields of physics/optics or physical chemistry.

In order to characterize the performance of our arrangement, we present a full characterization of the optical focus and report on the thickness and refractive index of nanometric material layers produced by ultramicrotomy. We also describe the application of our setup for characterizing the fluorescence radiation emitted by a crystalline thin-film made of a molecular switch compound. Reflection measurements are also possible using a bifurcated fiber. For validation of the spectrometer, we compare spectra measured for a solid state wavelength standard and for dye solutions with those measured in a classical two-beam spectrophotometer. These first results demonstrate the versatile application possibilities of our forthright optical arrangement.

II. OPTICAL AND MECHANICAL DESIGN

We call our design a *microspectrometer;* this shall not be confused with some miniaturized conventional grating spectrograph. The setup is depicted in Fig. 1(a). The light source is a deuterium-tungsten halogen lamp[7] covering a spectral range from 215 nm to above 1030 nm. The detector

for the light transmitted through the sample is a fiber-coupled miniature grating spectrograph[7] with a wavelength range from 200 to 1030 nm and an optical resolution of 2.0 nm (full width at half maximum, FWHM). The spectrograph uses a 500 lines/mm grating blazed at 250 nm to ensure high efficiency in the UV and a 25 μm entrance slit. Both the light source and the detector are connected by means of 1 m long solarization-resistant optical fibers with a core diameter of 200 μm.[7] The microspectrometer consists of four 90° off-axis parabolic mirrors with an effective focal length of 80 mm each.[7] These mirrors have an outer diameter of 49.5 mm and the diamond-turned optical surface is covered with a protected aluminum coating. The back surface is perpendicular to the optical axis. The effective focal length and the diameter of the parabolic mirrors are matched to the numerical aperture of the optical fibers, $NA = 0.22$, corresponding to an opening angle of the emitted light of $\pm 12.7°$, such that the entire radiation is collected. The aperture of the optical fiber coming from the light source is located at the focus of the first parabolic mirror. Thus, a collimated beam is created upon reflection. This beam is then focused by the second parabolic mirror towards the sample. The light transmitted through the sample, or its fluorescence, is collected by the third parabolic mirror. This produces again a collimated beam, which is finally focused with the fourth parabolic mirror onto the entrance aperture of the optical fiber leading to the grating spectrograph.

All optical components of the microspectrometer are mounted in a mechanical cage system.[7] This simplifies the alignment of the two pairs of off-axis parabolic mirrors by providing mechanical plates that are intrinsically parallel to each other. Mounting the back surfaces of the parabolic mirrors perpendicularly to the rail system provides a sufficient alignment for the here reported purpose. The remaining degree of freedom of the parabolic mirrors, rotation about the optical axis, is defined by alignment pins in the rear surface of the mirrors and corresponding holes in the mounting plates. These holes can easily be produced mechanically with sufficient accuracy. Thus, each pair of mirrors forms an enclosed and mechanically fixed unit that does not need to be adjusted after an initial alignment. The separation between the illuminating and the collecting mirror pairs can be adjusted in order to compensate for optical path length changes if thick samples are studied, for example 10 mm absorption cuvettes. The remaining alignment work involves the positioning of the exit and entrance apertures of the two optical fibers. Optomechanical XY translators within the cage system allow the precise positioning of the end of the optical fibers and movement along the light's propagation direction is achieved by sliding the XY translators along the rails of the optical cage system. The latter adjustment is not as precise as the sideways movements, but found to be well sufficient in the experiment. Once pre-aligned, the system can further be optimized by maximizing the detected intensity in the grating spectrograph.

Between the second and the third parabolic mirror, there are 89 mm of clear space. This is where the sample is located. For convenience in adjusting, the sample is mounted on a three-axis linear translation stage (XYZ), such that it can be adjusted precisely with respect to the focal spot of the light. If necessary, the positioning of the sample can be monitored with a CMOS camera equipped with a macro lens positioned at a 45° angle above the incident microspectrometer beam.

III. SPECTRALLY-RESOLVED FOCUS CHARACTERIZATION

Figure 1(b) shows the effective spectrum of the deuterium-tungsten halogen lamp as measured through the microspectrometer setup in the grating spectrograph. This trace represents the usable spectral range and spans a wavelength interval from 215 to 1030 nm. When the microspectrometer is properly aligned and no sample is inserted, the lamp is intense enough to limit the exposure time of the spectrograph to about 1 ms; for any longer exposure time, the detector will saturate. This demonstrates the excellent throughput efficiency of the setup, minimizing the measurement time and allowing to study samples with rather high optical densities. To measure transmission spectra, the detected spectrum is once recorded with the sample and once without; for dye solutions it is preferable to insert an identical cuvette with just the solvent.

In order to verify the proper alignment and the focusing performance of the microspectrometer, a camera was placed at the location of the sample. By translating it along the beam axis while monitoring the beam profile, the location of the focus can be found. The beam profile at this position is shown in Fig. 1(c). The profile is circular and has a flat-top profile, revealing the intensity

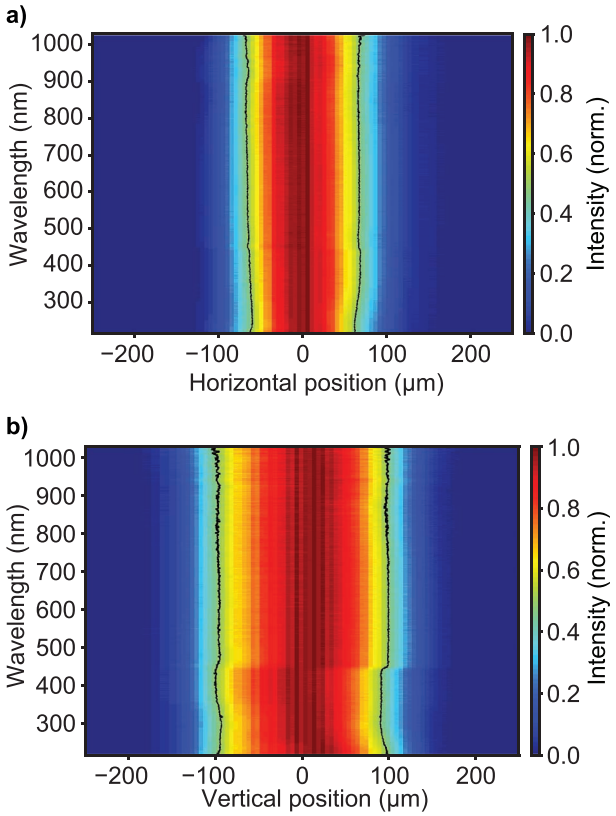

FIG. 2. Intensity profile obtained by knife-edge characterization of the focal spot for each wavelength individually. (a) Scan along the horizontal axis; (b) scan along the vertical axis. The black lines indicate the positions at which an intensity of half the maximum value is reached for each wavelength.

distribution at the exit aperture of the optical fiber coming from the lamp. The spot diameter is slightly below 200 μm (FWHM), as expected for a fiber core diameter of 200 μm and the 1:1 imaging system presented here.

The camera used to record the spot shown in Fig. 1(c) is sensitive over a wide spectral range (190–1100 nm). Hence the measured beam profile is spectrally integrated and provides no chromatic information about the focal spot. To obtain spectrally resolved information about the focus quality, knife-edge measurements[8] were performed. A razor blade was mounted at the location of the sample on the XYZ translation stage. It was then scanned across the focal spot, and for each position of the blade a transmission spectrum was recorded. We denote the beam's intensity profile at the plane of the traveling knife-edge with $I_\lambda(x, y)$ for a probe wavelength λ. The measured power P at the detector can be written as

$$P(x, \lambda) = \int_x^\infty dx' \int_{-\infty}^\infty dy' I_\lambda\left(x', y'\right), \tag{1}$$

where x indicates the position of the knife-edge. This neglects diffraction effects at the edge of the blade and assumes that the blade is moved through the beam along the positive x-direction. Differentiation of $P(x, \lambda)$ with respect to x provides a visualization of the beam profile along x. Two sets of knife-edge measurements were performed, one in the horizontal and one in the vertical direction.

The results are shown in Fig. 2. A 9-point running average along the position axis was used to smooth the data. For each wavelength, the black lines in Fig. 2 show the positions where the intensity drops to half its maximum value. From these numbers the FWHM width of the beam was calculated, resulting in values of (131 ± 3) μm in the horizontal direction and (193 ± 4) μm in

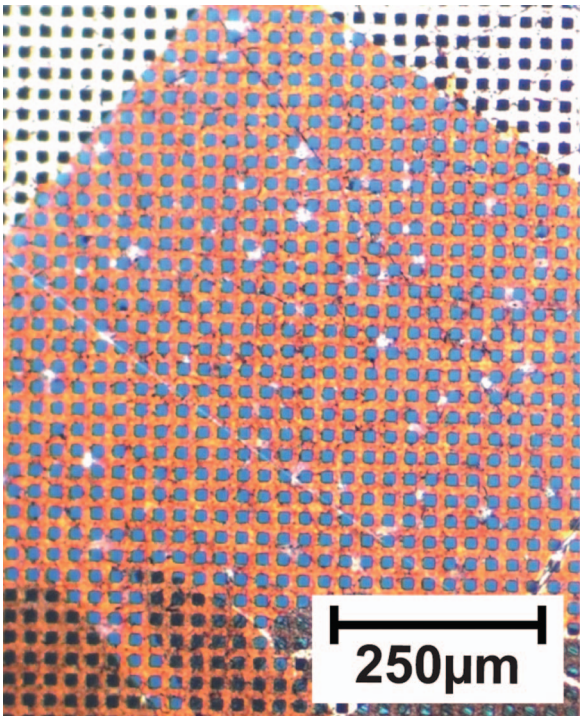

FIG. 3. 30-nm thick film of epoxy resin (bluish) on a gold support mesh.

the vertical direction. The center positions, half way between the half maximum points, drift only by ± 1 μm and ± 2 μm in the horizontal and vertical directions, respectively. These knife-edge measurements demonstrate that the focal spot at the sample location is very homogeneous with respect to the wavelength; all wavelengths reach the same spot and all have a similar beam diameter below 200 μm. The slight deviations between the knife-edge measurement and the wavelength-integrated camera measurement can be attributed to a slightly different position along the beam in the two experiments.

IV. THIN-FILM TRANSMISSION SPECTROSCOPY

The interaction of light with a sample can be decomposed into three primary components: transmission, reflection and absorption. The microspectrometer directly measures transmission, but often one is interested in the other quantities. Here we show an example of how our setup can be applied to determine the thickness and refractive index of a series of 25–250 nm thick films produced by ultramicrotomy for study with ultrafast electron microscopy and diffraction. Our test material is an epoxy resin (Araldite CY212), which is a useful compound for embedding materials prior to cutting them by ultramicrotomy. We produced a series of thin-films with increasing thickness and mounted them on transmission electron microscopy meshes with 2000 lines per inch (12.7 μm period). A film with a thickness of about 30 nm is shown in Fig. 3 (bluish color). The transmission data for the pure resin films was obtained by recording a transmission spectrum of the resin with mesh and dividing this data by the transmission spectrum of the uncovered parts of the same mesh, for each sample thickness.

Figure 4 shows a selection of the recorded transmission spectra. The spectra for different film thicknesses (not known a priori) differ strongly in shape and show varying fringes and minima. This is a result of optical interference, which is significant for film thicknesses that are similar to the optical wavelength.[9] Typical lamps have a coherence length of many micrometers[9,10] and a large number of reflections forth and back must hence be considered; see for example the text book by Born & Wolf.[9]

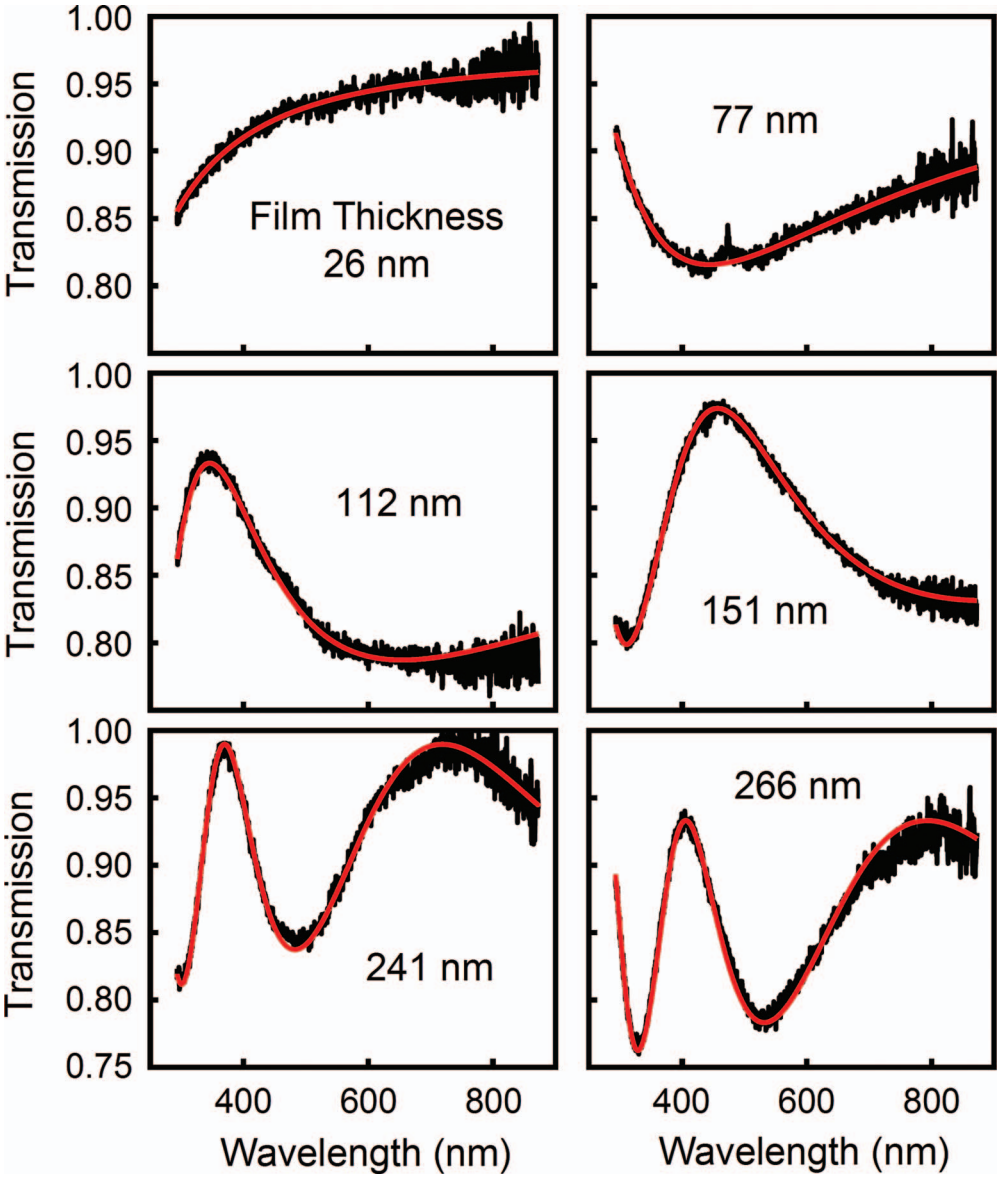

FIG. 4. Transmission spectra of epoxy resin thin-films. The black traces show the measured data and the red line indicates a least-square fit using a Sellmeier model for the complex refractive index of the material. The indicated thickness values are the result of the fit.

Obtaining the complex refractive index $\hat{n}(\lambda) = n(\lambda)(1 + i\kappa(\lambda))$ from thin-film measurements is nontrivial. Without any prior knowledge of $n(\lambda)$ and $\kappa(\lambda)$, it is impossible to retrieve them from a single transmission measurement $T(\lambda)$. At least two independent measurements are necessary, for example a combined transmission and reflectance measurement in the so-called (R, T) method[11] or alternatively a series of transmission measurements for different thicknesses.[12] However, under the assumption of a model for the optical properties of the thin-film, it is possible to calculate $n(\lambda)$ and $\kappa(\lambda)$ from a single transmission measurement.[13]

Here we apply this approach by modeling the refractive index of the thin-film by a Sellmeier equation $n(\lambda)$ with two free parameters c_1 and c_2 using $n(\lambda) = \sqrt{1 + \frac{c_1\lambda^2}{\lambda^2 - c_2}}$. The resin does not show any distinct absorption features in the wavelength range under investigation. We therefore approximate the imaginary part of the refractive index, i.e. the absorption, by $n\kappa(\lambda) = 0$. For each measured transmission spectrum, the thickness of the film as well as an offset compensating for

potential inaccuracies in the normalization of the mesh's transmission and for scattering losses are determined with a least-square fitting routine, while globally keeping a common model for the refractive index described by the parameters c_1 and c_2.

The resulting fits are shown as red lines in Fig. 4 and reproduce the measured transmission spectra quite well. The obtained thickness values span the range from 26 to 266 nm, which is consistent with the expectations from the ultramicrotomy process. The retrieved parameters in the Sellmeier equation for the real part of the refractive index are $c_1 = 1.2$ and $c_2 = 0.017\ \mu\text{m}^2$. These results demonstrate that the microspectrometer is capable of providing good information about the optical properties of tiny thin-film pieces on electron microscopy meshes.

V. VALIDATION OF THE MICROSPECTROMETER WITH REFERENCE SUBSTANCES

Ideally, the new microspectrometer should have a high precision in the wavelength scale and a good photometric accuracy in addition to the capability to measure spectra in tiny volumes. To validate the setup, we performed reference measurements in parallel with the microspectrometer and a commercial dual-beam scanning spectral photometer (Lambda 750, Perkin Elmer).

The first sample to be compared is a F1 holmium oxide glass-filter (HellmaAnalytics) displaying sharp absorption lines at precisely known wavelengths. The spectrum measured in the two instruments (see Fig. 5(a)) matches very well and we find a wavelength precision of better than 1 nm over the full range from 270 to 700 nm. Recording the spectrum in the microspectrometer only takes a fraction of a second due to the multi-channel detection, while scanning the commercial spectrophotometer takes some minutes. Still the spectrum recorded with our new setup displays a well sufficient signal-to-noise ratio (see red curve) to reproduce the trace from the standard instrument (blue curve, offset for clarity).

The photometric accuracy can be better judged from the absorption spectrum of dyes in solution, as these display very broad features. As an example we chose the laser dye Phenoxazone 9 (Lambda Physik AG) dissolved in ethanol (see Fig. 5(b)). The two traces are nearly indistinguishable over the full spectral range. From this comparison and others, we find that the microspectrometer can safely be used up to an optical density of 2, equivalent to just 1% transmission. An accuracy of better than 1% is possible with proper referencing of the instrumental throughput.

VI. ONLINE MONITORING OF CHEMICAL KINETICS

The capability to record spectra within less than a second and from a very small cross section makes the microspectrometer ideal to monitor the progress of a photochemical process. We illuminated 4-*tert*-butylphenyl acetate (BPA) dissolved in cyclohexane with 270 nm light at a power of 1.65 mW to convert it to 4-*tert*-butyl-2-hydroxyacetophenone (BOHA) by a photo-Fries arrangement.[14] The UV absorption of BPA is very weak and limited to the range below 280 nm. BOHA has a fairly strong absorption at 335 nm and down in the 250 nm range. The sample absorption was monitored every 30 seconds for 1 hour (see Fig. 5(c)). Clearly the increasing BOHA signatures are seen and allow for the quantitative determination of the reaction progress. In this 1 hour illumination already the major part of the sample is converted and the new signatures start to saturate. Due to the possibility to simultaneously illuminate and measure the spectrum, the photochemistry can be followed extremely easily and precisely without having to Transfer The Sample Repeatedly To A Spectrophotometer.

VII. FLUORESCENCE MEASUREMENTS

In addition to the transmission measurements described above, the microspectrometer can also be used efficiently for determining fluorescence spectra of small samples or the position dependence of the fluorescence spectrum. This is facilitated by the good detection efficiency of the microspectrometer for any light originating from the focal spot between the second and third parabolic mirror. In this type of spectroscopy, it is required to calibrate the absolute detection efficiency of the fiber spectrograph in dependence on wavelength and polarization, for example

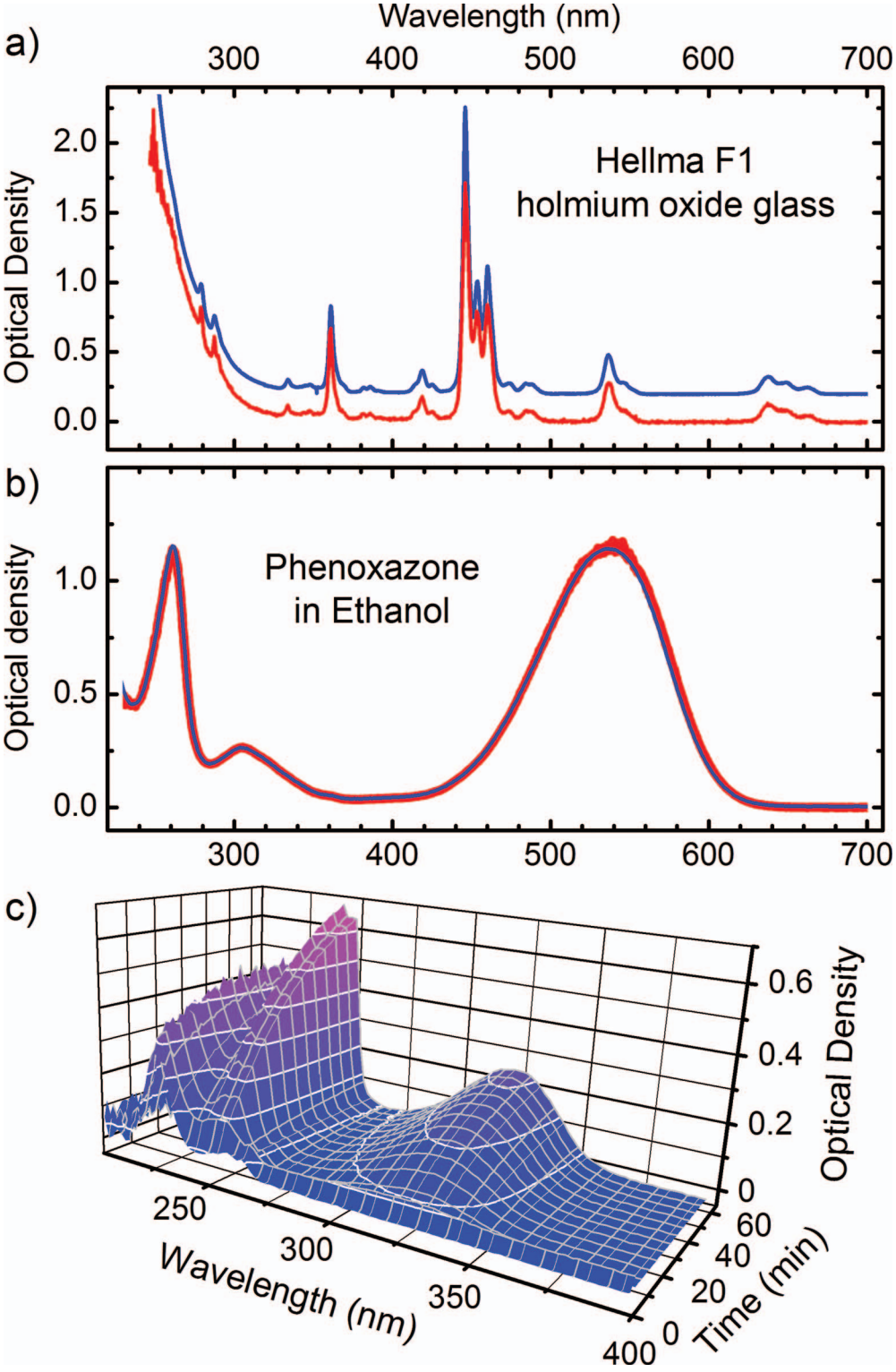

FIG. 5. (a–b) Comparison of the transmission spectrum measured with the microspectrometer (red traces) and a commercial spectrophotometer (blue traces). (a) F1 holmium oxide glass-filter; the traces are plotted with an offset. (b) Solution of Phenoxazone 9 (Lambda Physik AG) dissolved in ethanol in a 10 mm cuvette. (c) Application of the microspectrometer for chemical kinetics: Temporal evolution of a photo-Fries rearrangement according to Ref. 14.

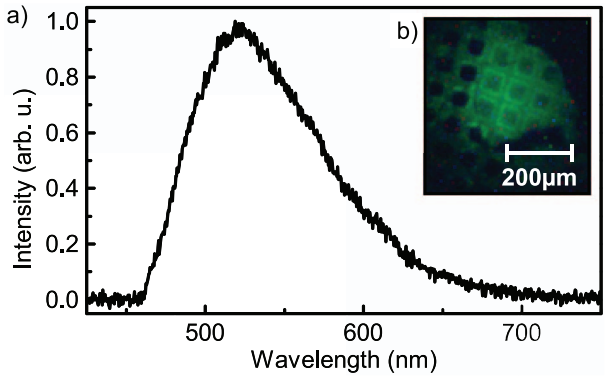

FIG. 6. (a) Fluorescence spectrum of a thin-film crystalline layer of N-(triphenylmethyl)-salicylidenimine as recorded with the microspectrometer. (b) The film of 50 nm thickness and diameter of 200 μm was excited by femtosecond laser pulses at 400-nm wavelength.

using a thermal black-body light source. For initiating fluorescence, the accessible mechanical construction of the microspectrometer offers many possibilities for illumination of the sample with excitation radiation. Figure 1 depicts the here applied option,using an excitation beam derived from a femtosecond laser (dotted lines). The polarization and intensity of the incident light can be varied by means of a polarizer and a wave-plate. Likewise, the polarization properties of the fluorescence can be analyzed using a broadband nanoparticle polarizer[7] in the detection path. Stray light from the excitation beam can be excluded from being measured by using apertures and wavelength filters; the space between the third and fourth mirror offers a collimated beam and ample space for such application-specific modifications.

As an example, we report the fluorescence spectrum of a 50-nm thick single-crystalline thin-film of N-(triphenylmethyl)-salicylidenimine[15] prepared by ultramicrotomy for use in diffraction.[16] This compound is a molecular switch based on an ultrafast excited-state intramolecular proton transfer mechanism.[17] The investigated sample has a diameter of approximately 200 μm and was mounted at the focal point of the third parabolic mirror. It was excited by the second harmonic of a Ti:sapphire laser with 800 μW of femtosecond laser pulses at a central wavelength of 400 nm. Stray light was blocked by a long pass filter suppressing wavelengths below 465 nm.[7] Figure 6(a) shows the measured fluorescence spectrum peaking at approximately 520 nm. Just a few seconds of integration time in the microspectrometer are sufficient to obtain the reported spectrum from the μm-sized and nm-thin emission volume (see Fig. 6(b)). The obtained spectrum agrees reasonably with an independent fluorescence measurement of a powder sample in KBr matrix excited with incoherent light at 350-nm wavelength. However, the polarization-dependent measurements made possible by our setup reveal a strongly orientation-dependent excitation efficiency and a polarized fluorescence output at a surprising angle with respect to the main axis of the molecules. These results will be analyzed elsewhere, but here demonstrate the capability of the microspectrometer for complex polarization studies of fluorescence from micrometer-sized and nanometer-thick crystals. The study of liquids is achievable by combining the microspectrometer with a fiber-coupled micro-fluid cell such as used in nuclear magnetic resonance.[18]

VIII. REFLECTANCE MEASUREMENTS

The microspectrometer is also suitable for reflectance measurements. This is of particular importance, as it allows the investigation of nontransparent samples, for example laser mirrors and their damaged spots. The main challenge is to separate the incident light from the reflected light. We chose to use a bifurcated optical fiber assembly,[7] in which two optical fibers are combined such that their cores lie extremely close to each other at a common mountable surface. This fiber is placed before the first parabolic mirror. One of the two arms of the bifurcated fiber is connected to the light source and the other one to the grating spectrograph. The parabolic mirrors three and four

are not in use. Since the two fiber cores are directly adjacent with a separation of about 200 μm, it takes only a small deviation from normal incidence on the sample to couple the reflected light into the other fiber. For calibration of the absolute spectral reflectivity, one can apply a reference sample, for example a metal surface or a set of dielectric mirrors of well-known reflectivity. The calibration mirror and the sample must be carefully placed along the z direction in the focus of the lamp, in order to obtain a comparable coupling efficiency of the reflected light. Occasionally there is some cross talk between the fibers, i.e. lamp light going directly into the grating spectrograph without hitting the sample. Although such effects can degrade the quantitative analysis of absolute intensities, we found experimentally from the example of a quasicrystal surface that the spectrally resolved reflectivity of μm-sized areas can at least be recorded qualitatively, allowing to identify spectral features of reflection processes on the micrometer scale.

IX. OUTLOOK AND CONCLUSIONS

The microspectrometer can be further improved, if necessary. The spatial resolution can be increased by using a smaller fiber for the light source, at cost of integration time, and/or by choosing de-magnifying parabolic optics with larger size or shorter focal length, at cost of working distance. For example, a 20-μm spot can be produced by combining a 40-μm fiber with focusing parabolic mirrors with a focal length of 40 mm. Measurements can also be performed on samples that are smaller than the focus area, at the cost of a reduced signal-to-noise. In this way, for example, we could successfully characterize the thickness of 50-μm-sized flakes of N-(triphenylmethyl)-salicylidenimine using the 200-μm-sized focus area characterized in Fig. 2. The spectral range of our setup can be extended by using a more broadband lamp and broader detector; the UV-enhanced metal-coated parabolic mirrors already have sufficient reflectivity.

In conclusion, the presented design of a microspectrometer setup combines 200-μm spatial resolution over the entire single-measurement range of 215–1030 nm with a high sensitivity. The mechanical construction requires little or no day-to-day alignment and forms a practical base for transmission, absorption, reflectivity, fluorescence and refractive index spectroscopy of tiny and ultrathin samples. We have given a detailed description of the quantitative capabilities, the attainable sensitivity and the precision possible with proper alignment and calibration. The reported examples should allow the interested scientists to assess whether such a setup can indeed resolve their questions and what quality of measurement to expect. This should not only contribute to avoiding futile efforts and investments, but also encourage researchers to make quantitative measurements where they were limited to qualitative observations so far.

ACKNOWLEDGEMENTS

We thank F. H. J. Hinzpeter and C. F. Sailer for preliminary experimental work, A. Lewanowicz for providing molecular crystals and M. Hoheneder for help with polarization-scanned fluorescence measurements. This work was supported by the Deutsche Forschungsgemeinschaft (DFG) through the Cluster of Excellence: Munich-Centre for Advanced Photonics, the Rudolf-Kaiser-Stiftung, the European Research Council and the International Max Planck Research School of Advanced Photon Science.

[1] David J. Flannigan and Ahmed H. Zewail, "4D electron microscopy: Principles and applications," Accounts of Chemical Research **45**(10), 1828–1839 (2012).
[2] Germán Sciaini and R. J. Dwayne Miller, "Femtosecond electron diffraction: heralding the era of atomically resolved dynamics," Reports on Progress in Physics **74**(9), 096101 (2011).
[3] Peter Baum, "On the physics of ultrashort single-electron pulses for time-resolved microscopy and diffraction," Chemical Physics **423**(0), 55–61 (2013).
[4] Goerg H. Michler and Werner Lebek, *Ultramikrotomie in der Materialforschung* (Hanser Verlag, München, 2004).
[5] Maximilian Eichberger, Marina Krumova, Helmuth Berger, and Jure Demsar, "Sample preparation methods for femtosecond electron diffraction experiments," Ultramicroscopy **127**(0), 9–13 (2013).
[6] L. S. Wong, F. Birembaut, W. S. Brocklesby, J. G. Frey, and M. Bradley, "Resin bead micro-uv - visible absorption spectroscopy," Analytical Chemistry **77**(7), 2247–2251 (2005).

[7] We refrain from mentioning the specific manufacturers in our setup, since emphasis of this paper is on general optical design and performance studies. Similar products from diverse vendors seem equally suitable for the present purpose.
[8] Marcos A. de Araújo, Rubens Silva, Emerson de Lima, Daniel P. Pereira, and Paulo C. de Oliveira, "Measurement of Gaussian laser beam radius using the knife-edge technique: improvement on data analysis," Applied Optics **48**(2), 393–396 (2009).
[9] Max Born and Emil Wolf, *Principles of Optics: Electromagnetic Theory of Propagation, Interference and Diffraction of Light* (Pergamon Press, 1970) 4th edition.
[10] Ekbert Hering, Rolf Martin, and Martin Stohrer, *Physik für Ingenieure*. (Springer, Berlin, 2012), 11th edition.
[11] P.-O. Nilsson, "Determination of optical constants from intensity measurements at normal incidence," Applied Optics **7**(3), 435–442 (1968).
[12] R. A. Hazelwood, "Derivation of optical constants from transmission measurements alone–applied to $MoSe_2$," Thin Solid Films **6**(5), 329–341 (1970).
[13] Dirk Poelman and Philippe Frederic Smet, "Methods for the determination of the optical constants of thin films from single transmission measurements: a critical review," Journal of Physics D: Applied Physics **36**(15), 1850–1857 (2003).
[14] Stefan Lochbrunner, Martin Zissler, Johannes Piel, Eberhard Riedle, Anja Spiegel, and Thorsten Bach, "Real time observation of the photo-fries rearrangement," Journal of Chemical Physics **120**(24), 11634–11639 (2004).
[15] Renata Karpicz, Vidmantas Gulbinas, Aleksandra Lewanowicz, Mindaugas Macernis, Juozas Sulskus, and Leonas Valkunas, "Relaxation pathways of excited n-(triphenylmethyl)salicylidenimine in solutions," Journal of Physical Chemistry A **115**(10), 1861–1868 (2011).
[16] Friedrich O. Kirchner, Stefan Lahme, Ferenc Krausz, and Peter Baum, "Coherence of femtosecond single electrons exceeds biomolecular dimensions," New Journal of Physics **15**(6), 063021 (2013).
[17] Christian Schriever, Stefan Lochbrunner, Armin R. Ofial, and Eberhard Riedle, "The origin of ultrafast proton transfer: Multidimensional wave packet motion vs. tunneling," Chemical Physics Letters **503**(1–3), 61–65 (2011).
[18] C. Feldmeier, H. Bartling, E. Riedle, and R. M. Gschwind, "LED based NMR illumination device for mechanistic studies on photochemical reactions - versatile and simple, yet surprisingly powerful," Journal of Magnetic Resonance **232**, 39–44 (2013).